Macromolecular Diffusion of Biological Polymers Measured by Confocal Fluorescence Recovery after Photobleaching

Philip Gribbon and Timothy E. Hardingham
Wellcome Trust Centre for Cell Matrix Research, School of Biological Sciences, University of Manchester, Manchester M13 9PT, England

ABSTRACT Fluorescence recovery after photobleaching with an unmodified confocal laser scanning microscope (confocal FRAP) was used to determine the diffusion properties of network forming biological macromolecules such as aggrecan. The technique was validated using fluorescein isothiocyanate (FITC)-labeled dextrans and proteins (molecular mass 4–2000 kDa) at 25°C and with fluorescent microspheres (207 nm diameter) over a temperature range of 5–50°C. Lateral diffusion coefficients (D) were independent of the focus position, and the degree and extent of bleach. The free diffusion coefficient (D_o) of FITC-aggrecan determined by confocal FRAP was $4.25 \pm 0.6 \times 10^{-8}$ cm^2 s^{-1}, which is compatible with dynamic laser light scattering measurements. It appeared to be independent of concentration below 2.0 mg/ml, but at higher concentrations (2–20 mg/ml) the self-diffusion coefficient followed the function $D = D_0 e^{-Bc}$. The concentration at which the self-diffusion coefficient began to fall corresponded to the concentration predicted for domain overlap. Multimolecular aggregates of aggrecan (~30 monomers) had a much lower free diffusion coefficient ($D_o = 6.6 \pm 1.0 \times 10^{-9}$ cm^2 s^{-1}) but showed a decrease in mobility with concentration of a form similar to that of the monomer. The method provides a technique for investigating the macromolecular organization in glycan-rich networks at concentrations close to those found physiologically.

INTRODUCTION

In most biological tissues, the extracellular matrix (ECM) defines the biomechanical properties and determines its architecture and form (Laurent, 1995). The ECM contains fibrillar and nonfibrillar components that combine to form a composite matrix (Mow et al., 1989). How the macromolecules that form the ECM interact to determine the properties of whole tissues is only partly understood (Winlove and Parker, 1995). The highly polyanionic glycosaminoglycans are important nonfibrillar components that frequently occur at high concentration in the ECM and have great influence on the movement of solutes and water between the tissue and the circulation, thereby influencing the access to cells of nutrients, metabolites, cytokines, hormones, and enzymes (Grodzinsky, 1983). This local environmental regulation may have important consequences for cellular functions, especially within tissues with a large expanded ECM, such as cartilage.

Many biophysical techniques are available for the study of solution properties of macromolecules (Janmey, 1993), but few are appropriate for the investigation of properties at high concentration, or with complex mixtures such as those found in the ECM in vivo. However, fluorescence recovery after photobleaching (FRAP) is a technique that has been used to investigate molecular mobility within cells and membrane systems in situ. The diffusion of FITC-labeled macromolecules measured by FRAP determines a lateral diffusion coefficient (Axelrod et al., 1976). In concentrated biopolymer solutions, as investigated in this study, this measurement constitutes a long-time self-diffusion coefficient (Imhof et al., 1994) that describes the motion of a polymer probe through a polymer matrix (Phillies, 1989). In the limit of zero tracer concentration, when interactions between particles can be neglected, the particle Brownian motion is described by the free diffusion coefficient (Imhof et al., 1994). In this study we have developed the use of an unmodified confocal laser scanning microscope (CLSM) to study diffusion in concentrated solutions and have applied it to investigate the properties of aggrecan, a high-molecular-weight proteoglycan, with more than 100 chondroitin sulfate and keratan sulfate chains attached to a protein backbone, that forms networks in solution at concentrations comparable to those found in tissues. The technique developed is applicable to the study of tracer diffusion in any bulk polymer system and may therefore help to give new insights into a broad range of studies

MATERIALS AND METHODS

Preparation and characterization of aggrecan and FITC aggrecan

Aggrecan and its link-stable aggregate were prepared from fresh porcine laryngeal cartilage (Hardingham, 1979). Aggrecan was extracted from the tissue in 4 M guanidine hydrochloride containing proteinase inhibitors, and aggregates were reformed and purified by cesium chloride density gradient ultracentrifugation under associative conditions. Monomeric aggrecan was prepared by a second cesium chloride density gradient ultracentrifugation step under dissociative conditions (Hardingham, 1979). Both preparations were dialyzed, freeze dried, and stored at −20°C. Molecular weights were determined by size exclusion column chromatography (16 × 700 mm, 0.4 ml/min, Sephacryl S-500; Pharmacia, Uppsala, Sweden), with online multiangle laser light scattering and a differential refractometer (Dawn DSP; Wyatt Technology, Santa Barbara, CA) (Reed, 1996). Molecular weights

Received for publication 20 October 1997 and in final form 11 May 1998.

Address reprint requests to Dr. Timothy E. Hardingham, Wellcome Trust Centre for Cell Matrix Research, School of Biological Sciences, University of Manchester, 2.205 Stopford Building, Oxford Road, Manchester M13 9PT, England. Tel.: 44-161-275-5511; Fax: 44-161-275-5082; E-mail: tharding@man.ac.uk.

0006-3495/98/08/1032/08 $2.00

were calculated using a second virial coefficient of 4.0×10^{-4} (ml $\times$ mol/g^2) and a refractive increment (dn/dc) of 0.16 (ml/g) (Kitchen and Cleland, 1978). On Sephacryl S-500 (Pharmacia), aggrecan gave a weight-averaged molecular weight (M_w) of $2.6 \pm 0.3 \times 10^6$ (mean $\pm$ SE, $n = 4$), a number-averaged molecular weight (M_n) of $2.1 \pm 0.3 \times 10^6$ (mean $\pm$ SE, $n = 4$), and a radius of gyration (R_G) of 62.8 $\pm$ 1.7 nm (mean $\pm$ SE, $n = 4$). Chromatography of the aggregate preparation on Sephacryl S-1000 (Pharmacia) separated a link-stable aggregate fraction in the V_o from free monomer (Hardingham, 1979). M_w was $74.6 \pm 3.2 \times 10^6$ (mean $\pm$ SE, $n = 2$), M_n was $71.9 \pm 6.8 \times 10^6$ (mean $\pm$ SE, $n = 2$), and R_G was 234 $\pm$ 21 nm (mean $\pm$ SE, $n = 2$).

Aggrecan monomer (5 mg/ml) was covalently labeled with fluorescein isothiocyanate (FITC) (0.05 mg/ml) in 0.1 M carbonate-bicarbonate buffer, pH 9.0, for 18 h at 4°C, and freeze dried after free FITC was removed by exhaustive dialysis against deionized water. The aggregate preparation was similarly labeled with FITC and then fractionated on Sephacryl S-1000 to isolate the aggregate. Spectrofluorometric (Jasco Instrument Corp., Japan) measurements on both preparations showed 2.5 mol FITC/mol aggrecan. Fluorescein was the fluorophore of choice because it readily photolyzes under relatively low illumination intensities (Chen et al., 1995). Size exclusion chromatography of the FITC-labeled preparations showed that the molecular weights were unaffected by the labeling procedure. A sample of FITC aggrecan was digested with chondroitinase ABC and keratanase, and size exclusion chromatography on Sepharose CL-6B confirmed that all of the fluorescence was retained with the protein core and not released with the glycosaminoglycan chains.

FITC-labeled aggrecan was freeze dried to constant mass, and solutions in phosphate-buffered saline (PBS) (0.01 M phosphate, 0.138 M NaCl, 0.0027 M KCl) were prepared by weight. Samples at 100 μg/ml to 20 mg/ml were equilibrated for 48 h at 4°C and centrifuged at $3000 \times g$ for 30 min before experiments. Sample concentrations were checked using the 1,9-dimethylmethylene blue assay, with chondroitin sulfate C (Sigma, Poole, England) as a standard (Ratcliffe et al., 1988). FITC concentration was between 0.05 μg/ml and 15 μg/ml, which is unlikely to show fluorescence self-quenching (Cutts et al., 1995).

Dynamic light scattering measurements

Aggrecan solutions in PBS at a concentration from 0.8 to 1.9 mg/ml were equilibrated for 48 h at 4°C, centrifuged, and then filtered through a 0.2-μm filter into a quartz cell for the measurement of dynamic light scattering (DLS) (Malvern Instruments, 4700c). At each concentration four measurements were made, all at a scattering angle (θ) of 30° and at 25 $\pm$ 0.1°C. Data were analyzed by the method of cumulants (Li and Reed, 1991).

Fluorescent dextran, protein, and polystyrene microsphere standards

A range of FITC-dextrans (weight-averaged molecular mass 4.4–2000 kDa, polydispersity between 1.25 and 1.5, molar ratio FITC/glucose ~0.008; Sigma) were dissolved in PBS, and measurements were made at 0.1 mg/ml. For the 2000-kDa FITC-dextran, measurements were also made at five dilutions between 0.2 and 0.0125 mg/ml to determine the extent of intermolecular interactions (Poitevin and Wahl, 1988). Green fluorescent polystyrene microspheres (average diameter 207 nm; Duke Scientific, Palo Alto, CA) were used at 0.1% v/v in PBS. Bovine serum albumin (BSA), soybean trypsin inhibitor (SBTI), and FITC-insulin were obtained from Sigma. SBTI and BSA were labeled with FITC by the method described above. The FITC conjugation ratio was 1.0, 1.5, and 1.1 mol/mol for FITC-insulin, FITC-BSA and FITC-SBTI, respectively. Measurements on FITC-conjugated proteins in PBS were made at five dilutions between 0.2 and 0.0125 mg/ml. The concentration of all FITC-dextran and FITC-protein solutions was determined by dissolving known dry weights. Chromatography of protein and dextran solutions (2.0 ml/min, Hi-Trap; Pharmacia) confirmed the absence of unconjugated FITC. Further multi-angle laser light scattering chromatographic analysis of the BSA and FITC-BSA (Superose-12; Pharmacia) showed the preparation to be monomeric. Before confocal-FRAP experiments, all dextran and protein solutions were filtered (0.45 μm) and centrifuged for 30 min at $10{,}000 \times g$.

Development of confocal FRAP protocols

Photobleaching experiments were carried out using a confocal laser scanner (MRC-1000; BioRad, Hemel Hempstead, England) with an upright epifluorescence microscope (Optiphot 2; Nikon, Japan). The 488-nm line of a 100-mW argon ion laser was used for sample bleaching and fluorescence excitation. Emitted light was monitored at 520 nm. Samples (30 μl) were in a spherical cavity microscope slide (diameter 12 mm, maximum depth 280 μm) sealed under a coverslip and were equilibrated for 15 min on a temperature-regulated microscope stage (PE-60; Linkam Instruments, Tadworth, England), usually at 25°C. Typical settings for prebleach and recovery image scans were 0.3% of maximum laser power, a pixel size of 1.47 μm, and an optical zoom of 1.0. From the whole field (760×512 pixels) a square central region of side ω (typically 50 pixels, 73.5 μm) was selected for bleaching. A prebleach image of dimensions $8 \times \omega$ (400 pixels), centered on the bleach region, was then captured. Bleaching was at maximum laser power and the area was selected by the zoom control of the instrument. The minimum bleach scan time was 140 ms, although typical times were 540 ms. For recovery, the program reset the instrument to the prebleach configuration and a time series of up to 50 recovery images was collected, typically over 2–10 min. A final image was taken at a long time point, to confirm that recovery approached completion. For slowly diffusing samples, two or more images were collected at each time point and averaged to reduce noise. Because the recovery was monitored at 0.3% maximum laser power, the bleach and monitor scan times were equal, and the area monitored was 64 times the area of the bleach; even with up to 50 images, the energy per unit area delivered to the sample during recovery is very small (<0.24%) compared with that required for photobleaching. For the CLSM it has been demonstrated (Blonk et al., 1993) that recovery analysis in three dimensions reduces to the simpler two dimensional case, for low numerical aperture (NA) objectives and wide confocal apertures as used in these studies (×10 objective, numerical aperture 0.45, confocal aperture 5 mm).

Data analysis

In the development of FRAP analysis using a modified CLSM for investigating molecular mobility in cell membranes, Kubitscheck et al. (1994) presented a moments analysis of fluorescence recovery based on that outlined by Jain et al. (1990). Because this method of analysis does not rely on rapid switching between bleach and recovery modes, it is well suited for use with unmodified confocal FRAP. The derivation presented by Kubitscheck et al. (1994) established the relationship between the time development of the variance (second moment) of the radial distribution of the bleached fluorophore, $\mu_2(t)$, and the lateral diffusion coefficient, D, as follows:

$$\mu_2(t) = 4kDt + \langle x_0^2 \rangle + \langle y_0^2 \rangle \quad (1)$$

where t is time, k is the fraction of mobile species, and x_o and y_o are functions of the initial bleach geometry. Equation 1 shows that the time dependence of $\mu_2(t)$ can be used to determine D independently of any knowledge of the initial bleach geometry (provided that the mobile fraction k is determined). Kubitscheck et al. showed Eq. 1 to be valid for any symmetrical bleach geometry, including a rectangular bleach, which is most easily produced by the scanning action of a CLSM.

Sets of recovery images were analyzed by MPL (Microscope Programming Language, BioRad) programs linked to spreadsheet routines. To remove nonuniformities in illumination, floating point ratio images were generated by dividing each recovery image by the prebleach image, and ratio images were then spatially filtered. Potential problems due to sample convection in the image plane and scan beam mistracking were monitored

by means of a center-of-mass calculation to determine movement of the bleach center position. The center of the bleach was taken as the origin ($r = 0$), and the average fluorescence intensity at radial position r was calculated for all pixels within $0 < r < 3\omega$ (ω is the bleach width), to generate a set of radial intensity profiles, $I_i(r)$. The mean intensity M_i of pixels for $3\omega < r < 4\omega$ was found for each image i. The radial distribution of bleached fluorophores $B_i(r,t)$ was then defined as follows:

$$B_i(r, t) = M_i - I_i(r, t) \quad (2)$$

For each profile $B_i(r)$, the variance μ_2 of the radial distribution of photolyzed fluorophores was then defined as follows:

$$\mu_2(t) = \frac{\int_0^{3\omega} r^3 B_i(r, t)\mathrm{d}r}{\int_0^{3\omega} rB_i(r, t)\mathrm{d}r} \quad (3)$$

As presented, the moments analysis remains valid while all photolyzed molecules remain within 3ω of the bleach center (Kubitscheck et al., 1994). Simulations for a uniform circular bleach of diameter 75 μm showed that, for $D = 1 \times 10^{-6}$ cm^2 s^{-1}, 1% of photolyzed fluorophores exited $r < 225$ μm after 17 s (Soumpasis, 1983). However, for typical macromolecules with D values less than 1×10^{-7} cm^2 s^{-1}, a 1% loss of fluorophores from $r < 225$ μm is exceeded only after 150 s, allowing ample time for data acquisition.

For each experiment, the mobile fraction (k) was calculated from the corrected integrated intensity within the bleached region as recovery became complete. In the experiments reported here, recoveries were complete ($k = 1$). Lateral diffusion coefficients (D) were calculated from linear regression analysis of plots of $\mu_2(t)$ against t. Free lateral diffusion coefficients (D_0) were calculated by linear regression and extrapolation to zero concentration.

RESULTS

An initial evaluation showed that the MRC-1000 CLSM with an upright microscope was best suited to delivering maximum laser power to the sample. It gave good control of bleach geometry and allowed easy development of customized routines. The confocal FRAP experimental protocols were controlled by simple macro programs written in MPL. The range of lateral diffusion coefficients accessible to analysis by this confocal FRAP protocol can be extended by varying the bleach size. In Fig. 1, characteristic diffusion times (τ_c) are shown for a range of diffusion coefficients (D) versus the diameter (d) of a circular bleach, where $\tau_c = d^2/4D$ (Soumpasis, 1983). It should be noted that the typical dimension of the bleached area is much larger than that used in FRAP experiments on cell membranes, and this provides for long recovery times, even for molecules with relatively high lateral diffusion coefficients. The time scale of the experiments is long and the dimensions of the bleach and area of analysis are very large compared with molecular dimensions of the mobile species being investigated. The data are therefore insensitive to any mode of molecular mass redistribution (i.e., rotational or vibrational) other than lateral diffusion of the FITC-labeled molecules.

Validation of confocal FRAP protocol

Confocal FRAP experiments were carried out with FITC-dextran (260 kDa) in dilute solution (0.1 mg/ml) in PBS at 25°C with a square bleach (73.5 μm), and the diffusion coefficient was calculated from a time series of radially averaged normalized fluorescence intensity profiles (Fig. 2). In these initial studies it was noted that for slowly diffusing molecules, such as 260 kDa FITC-dextran, the predicted linear relationship between $\mu_2(t)$ and t is observed (Fig. 3 *A*). Having obtained good results with a high-molecular-weight FITC-dextran, the technique was tested on a lower-molecular-weight globular protein, bovine serum albumin. Linear regression analysis of the data shown in Fig. 3 *B*, at short times ($t < 40$ s), gave a D of 6.05×10^{-7} cm^2 s^{-1} for FITC-BSA, which compares well with published values (Johnson et al., 1995). However, as predicted for a more mobile species, the variance deviates from this linear behavior at longer times ($t > 40$ s). Data were therefore analyzed from the variance results in the initial linear section as reported by Kubitscheck et al. (1994).

To investigate whether measurements were affected by the distance into the solution of the confocal image, the diffusion of 207-nm microspheres was measured at seven positions between 50 μm and 180 μm from the coverslip and was found to be independent of position (two-tailed unpaired Student's t-test, comparison between D at 110 μm and D at all other positions, $N = 4$ for each condition). There was also found to be no dependence of the results with FITC-dextran (167 kDa) on the dimension of the bleach (two-tailed unpaired Student's t-test, comparison between D at $\omega = 75$ μm and D for 11 square bleach sizes between 30 μm and 300 μm, $N = 4$ for each condition).

The lateral diffusion coefficient was also measured as a function of increased bleach intensity as determined from the average bleached fluorescence intensity within $r < \omega/2$ of the prebleach and first postbleach images. For the FITC-

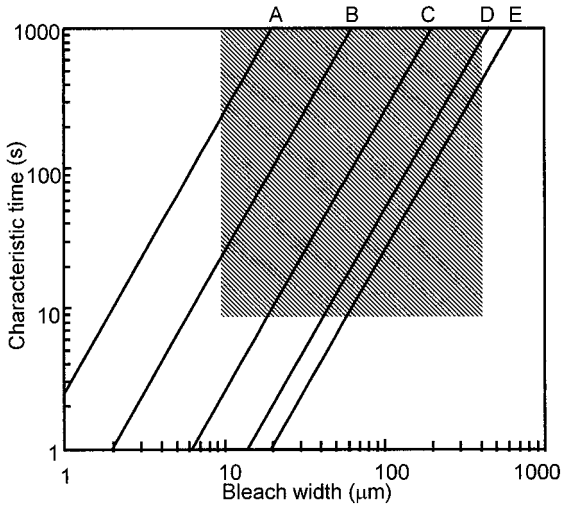

FIGURE 1 Theoretical plots calculated from expressions given by Soumpasis (1983), of characteristic diffusion time (s) as a function of bleach diameter (μm) for molecules with lateral diffusion coefficients. (*A*) 1×10^{-9} cm^2 s^{-1}. (*B*) 1×10^{-8} cm^2 s^{-1}. (*C*) 1×10^{-7} cm^2 s^{-1}. (*D*) 5×10^{-7} cm^2 s^{-1}. (*E*) 1×10^{-6} cm^2 s^{-1}. The shaded area shows the range of bleach dimensions and experimental times most suited to the confocal-FRAP protocol.

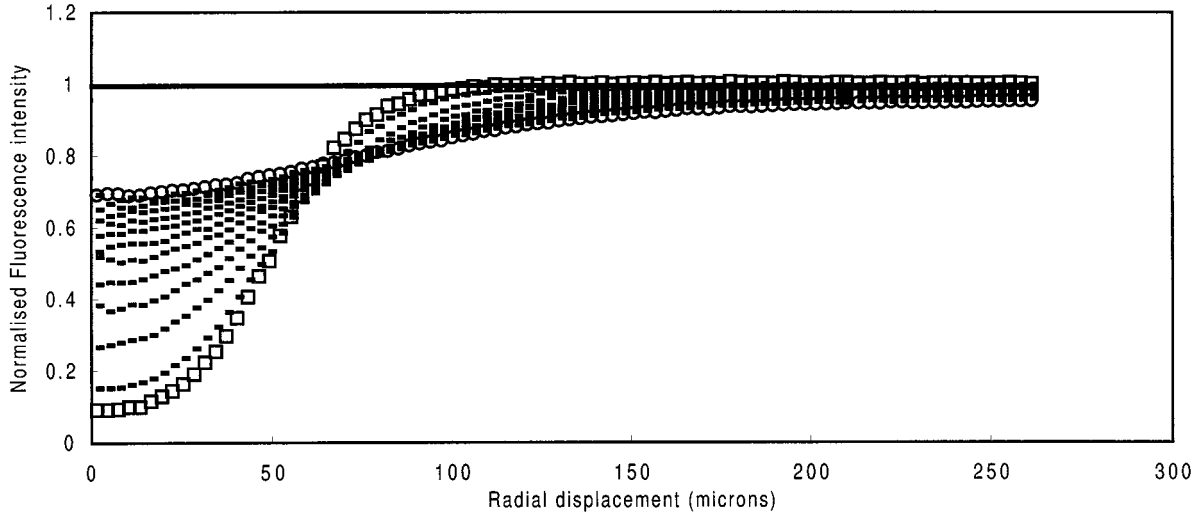

FIGURE 2 Time series of calculated radially averaged fluorescence intensity profiles (normalized) for a confocal-FRAP experiment with FITC-dextran (260 kDa) at 0.1 mg/ml. The first postbleach profile is at 3 s (■). Subsequent profiles are at 6-s intervals (-). The final profile is at 72 s postbleach (●). Mobile fraction = 1.00. Image dimensions 588 × 588 μm, bleach dimensions 73.5 × 73.5 μm.

dextran (167 kDa), D was independent of bleach intensity from 37.5% to 91% (two tailed unpaired Student's t-test, comparison between D for an 80% bleach intensity and D for 5 bleaches between 37.5% and 91%, $N = 4$ for each condition). However, for lower degrees of bleaching (<30%), there was insufficient image contrast for satisfactory data analysis.

Experiments were carried out on a range of FITC-dextrans of different molecular weights to investigate the correlation between the lateral diffusion coefficient and the weight-averaged molecular weight. Initially it was shown that for even the largest FITC-dextran fraction (2000 kDa), there was no detectable concentration dependence of the lateral diffusion coefficient. The calculated D_0 of 2000 kDa FITC-dextran was not significantly different from the lateral diffusion coefficients at five concentrations between 0.2 and 0.0125 mg/ml (two-tailed unpaired Student's t-test, $N = 4$). The lower-molecular-weight FITC-dextrans were therefore all investigated at 0.1 mg/ml. The results showed a linear relationship between log D (lateral diffusion coefficient) and log molecular weight (weight average) (Fig. 4). Power law relationships, i.e., $D = \alpha$ (molecular weight)$^{\beta}$, have been shown to apply to wide range of flexible polymers (Schmidt and Burchard, 1981). Values of $\alpha = 5.5 \times 10^{-5}$ and $\beta = -0.43$ were found in studies on dilute dextran solutions of between 20 kDa and 130 kDa (Amu, 1982). Analyzing the confocal FRAP results for FITC-dextran solutions between 4 kDa and 2000 kDa gave comparable results with $\alpha = 2.71 \times 10^{-5}$ and $\beta = -0.37$ (nonlinear least-squares fit, $R^2 = 0.996$). The differences in the values of α and β may be accounted for by differences in the degree of branching and polydispersity of the dextrans used in the two studies.

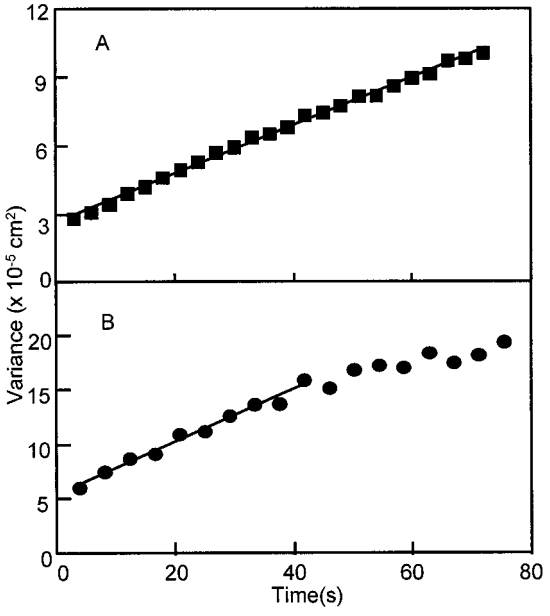

FIGURE 3 Second moment of the radial distribution of bleached fluorophore concentration, $\mu_2(t)$, versus time (t) for (A) FITC-dextran (260 kDa) and (B) BSA (67 kDa). Solid lines show a linear least-squares fit over $0 < t < 72$ s ($R^2 = 0.954$) for A, and over $0 < t < 42$ s ($R^2 = 0.984$) for B. All solutions were in PBS at 25°C.

The ability of the confocal FRAP technique to determine accurately lateral free diffusion coefficients, at a range of concentrations from 0.0125 to 0.2 mg/ml, was tested in experiments on FITC-labeled proteins (FITC-SBTI, FITC-insulin, FITC-BSA) at 25°C. The data compare well with published values obtained by other methods, corrected to 25°C in 150 mM NaCl (Table 1). The influence of temperature on lateral diffusion measurements was assessed by experiments with microspheres (207 nm) carried out over the temperature range 5°C to 50°C (Table 2). The diffusion coefficient was calculated as follows, for each temperature,

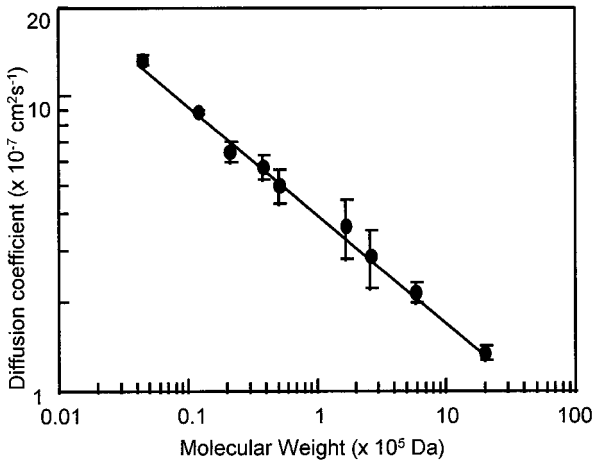

FIGURE 4 Lateral diffusion coefficients of FITC-dextran fractions of a range of molecular mass (4–2000 kDa). FITC-dextran concentration = 0.1 mg/ml. The vertical lines show ±1 standard deviation. The solid line shows a power-law fit to the data (see Results). Bleach protocols are as outlined in Fig. 2. All measurements were in PBS at 25°C ($N = 4$).

with the Stokes-Einstein approximation for the hydrodynamic behavior of an sphere:

$$D = \frac{\kappa T}{6\pi\eta R_h} \tag{4}$$

where κ is Boltzmann's constant, T is absolute temperature, η is the viscosity of 150 mM NaCl, and R_h is the hydrodynamic radius. The results showed no change in the diffusion coefficient after correction for changes in the viscosity of buffer and no evidence of interference from temperature instability, or convection within the samples. Thus there was good agreement between the results determined by confocal FRAP and those obtained by other established techniques for lateral diffusion coefficients over the range 1×10^{-6} to 1×10^{-8} cm^2 s^{-1}, and the technique was also applicable to temperature studies in the range 5°C to 50°C.

The concentration dependence of the self-diffusion of FITC-aggrecan

At low concentrations the self-diffusion of FITC-aggrecan showed no detectable concentration dependence below 2.0 mg/ml (Fig. 5). Linear extrapolation to zero concentration from results for $c < 1.6$ mg/ml gave a free diffusion coefficient (D_o) of $4.25 \pm 0.6 \times 10^{-8}$ cm^2 s^{-1} corresponding to an equivalent hydrodynamic radius (R_H) of 57 nm. The reduction in mobility above 2.0 mg/ml is consistent with the effects of domain overlap. For results above 2.0 mg/ml, a function of the type $D = D_0 e^{-Bc}$ was fitted by a nonlinear least-squares analysis. The extrapolation of this curve to zero concentration gave a D_o of 4.93×10^{-8} cm^2 s^{-1} and a B of 0.180 (ml/mg) ($R^2 = 0.989$) (Fig. 5). This D_o value is greater than that found by extrapolation of the results at low concentration and is greater than the z-averaged diffusion coefficient ($\theta = 30°$), calculated from DLS by the method of cumulants, which gave a D_o of $4.0 \pm 0.4 \times 10^{-8}$ cm^2 s^{-1}. The critical overlap concentration is predicted by the work of Phillips and Jansons (1990) to be 2.3 mg/ml, and this agreed with the results and is most apparent by replotting data (Fig. 6) relative to the D_o extrapolated from the low concentration results.

TABLE 1 Comparison of measured free diffusion coefficients, in PBS at 25°C, of FITC protein standards with previously published values

Protein	Molecular weight (kDa)	D_0 + SD ($\times 10^{-7}$ cm^{2}s^{-1})	Published D_0 ($\times 10^{-7}$ cm^{2}s^{-1})
Insulin	12	14.7 ± 1.3	16.8*
SBTI	21.6	8.8 ± 0.7	9.9*
BSA	67	5.8 ± 0.5	5.8–7.0#

Free diffusion coefficients were calculated by linear regression to zero concentration of data from at least four analyses of five protein concentrations between 0.2 and 0.0125 mg/ml. Published values were corrected to 25°C with the Stokes-Einstein equation.
**CRC Handbook of Biochemistry* (1968).
#Johnson et al. (1995), and references therein.

TABLE 2 Measured ($N = 4$) and calculated diffusion coefficients of 207-nm-diameter green fluorescent microspheres over a range of temperatures

Temperature (°C)	Lateral diffusion coefficient ± SD ($\times 10^{-9}$ cm^{2}s^{-1})	Calculated diffusion coefficient ($\times 10^{-9}$ cm^{2}s^{-1})
5	10.9 ± 2.3	12.7
12	16.3 ± 4.1	16.0
20	20.3 ± 6.3	20.4
25	22.4 ± 2.6	23.3
35	27.4 ± 6.3	29.8
50	45.7 ± 8.8	41.1

Diffusion coefficients were calculated with the Stokes-Einstein equation, assuming ideal hydrodynamic sphere behavior.

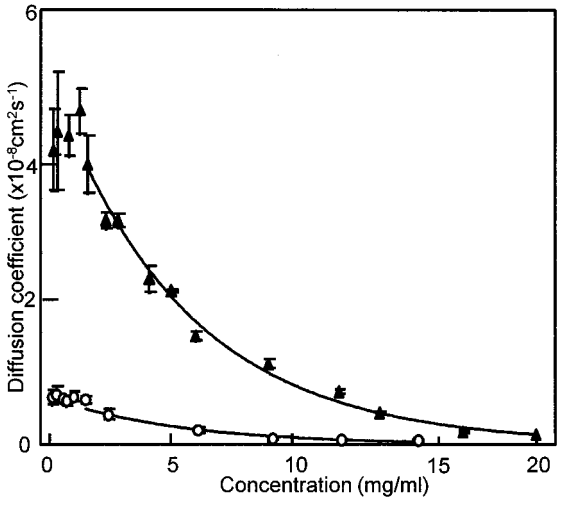

FIGURE 5 Lateral diffusion coefficient of aggrecan monomer (▲) and aggregate (○) at different concentrations. The vertical lines show ±1 standard deviation. The solid lines show the fitted exponential functions (see Results). All measurements were in PBS at 25°C ($N = 6$).

Over the concentration range investigated, the self-diffusion coefficients of the aggregate preparation were below those of the monomer preparation (Fig. 5). A linear least-squares fit to data below 1.0 mg/ml, for the aggregate, gave a D_o of $6.6 \pm 1.0 \times 10^{-9}$ cm^2 s^{-1} (R_H = 370 nm) and showed no detectable concentration dependence up to 1.5 mg/ml, after which it fell rapidly. The results for the aggregate were analyzed in a way similar to the analysis of the monomer. Fitting data for $c > 1.5$ mg/ml with $D = D_0e^{-Bc}$ gives a D_o of 6.6×10^{-9} cm^2 s^{-1} and a B of 0.187 (ml/mg) (R^2 = 0.950) (Fig. 5). The function agrees well with the data, and the predicted D_0, in contrast with the monomer, is similar to that found by linear extrapolation of the results at low concentration. The transition from a concentration-independent to a concentration-dependent fall in mobility is shown most clearly in a plot of D/D_o (Fig. 6).

DISCUSSION

In the adaptation of CLSM for FRAP analysis, there are some notable advantages over conventional FRAP systems (Bayley and Clough, 1995). A major advantage is that analysis with the CLSM based on imaging obviates the need for optical bench stability and alignment and makes the whole analysis more robust. Confocal imaging also avoids surface artefacts, and varying the degree of confocality permits data to be collected from increased volumes of those samples that are only weakly fluorescent. In this investigation of macromolecular properties in solution, there was also no need to restrict bleach areas (as is necessary in cell membrane studies), and thus it was possible to develop a technique using a CLSM without modification.

A disadvantage of the CLSM configuration is that it takes a longer time to switch from high-intensity bleach mode to low-intensity data collection than it does with non-CLSM equipment. However, this is not a problem with solution studies, as bleach recovery times can be adjusted to suit the macromolecule being investigated by increasing the bleach dimension. With ECM macromolecules, which are commonly of high molecular mass (>50 kDa), their translational diffusion coefficients are relatively low, and with a typical bleach (75 × 75 μm) taking 0.5–3.0 s, the recovery times are 30–3000 s. By appropriate manipulation of the bleach and recovery conditions (Fig. 1), the translational diffusion of both small tracer species and concentrated networks is open to investigation with confocal FRAP. The independence of D of bleach size and the focal plane within the sample volume agreed with studies on other configurations of FRAP using three-dimensional geometries (Imhof et al., 1994; Jain et al., 1990). The technique is thus well suited to investigating macromolecules forming networks with low lateral diffusion coefficients, as well as the mobility of low-molecular-weight probes within such networks.

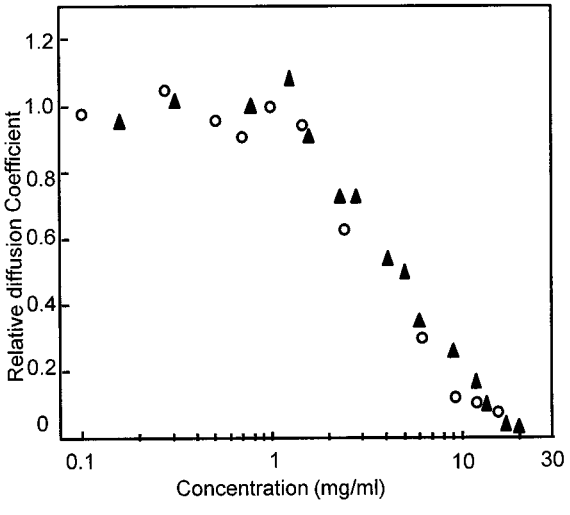

FIGURE 6 Concentration dependence of the relative diffusion coefficient of aggrecan monomer (▲) and aggregate (○). Results are as in Fig. 5. D_o values were calculated from linear extrapolation at low concentration. For all points, standard deviations lay between 0.14 and 0.22.

FRAP was not applied previously to aggrecan solutions, although other workers have reported light scattering and ultracentrifuge studies with dilute solutions (Harper et al., 1985). Dynamic light scattering studies at 25°C on a lower-molecular-weight aggrecan preparation (1.6×10^6) from bovine nasal cartilage reported that the translational diffusion coefficient as 5.8×10^{-8} cm^2 s^{-1} (Li et al., 1991), whereas studies on a higher-molecular-weight aggrecan preparation (3.0×10^6) from chick limb bud showed a diffusion coefficient of $4.13 \pm 0.38 \times 10^{-8}$ cm^2 s^{-1} (Ohno et al., 1986). These results are consistent with those reported here for 2.6×10^6 Da aggrecan. So, in the limit of zero concentration, the confocal FRAP method gives a lateral diffusion coefficient comparable to results from light scattering and analytical ultracentrifugation methods.

For aggrecan monomer samples at concentrations above 2 mg/ml, which are difficult to analyze by light scattering or analytical ultracentrifugation, confocal FRAP shows a strong concentration-dependent fall in mobility (Fig. 6). Predictions of polymer behavior in the concentrated entanglement-dominated regime (de Gennes, 1974; Hess, 1986) are available for linear but not branched polymers. However, empirically, at concentrations above that predicted for domain overlap, the results fit well to a function in the form $D = D_0e^{-Bc}$, which is equivalent to a stretched exponential model, $D = D_oe^{-Bc\nu}$, with $\nu = 1$ (Ogston et al., 1973; Phillies, 1989). From the results it is evident that aggrecan monomer mobility is restricted but not prevented at concentrations up to seven times that predicted for critical overlap. As the concentration of aggrecan monomer increases, there must be major contraction and/or interpenetration of the hydrodynamic domains. As interpenetration and consequent entanglement are likely to result in an increasingly immobile network as the concentration increases (Hess, 1986), the present results may imply that at high concentrations aggrecan domains mainly contract. This is also consistent with their properties in forming viscoelastic solutions but not gels at high concentration (Hardingham et al., 1987),

and it is supported by evidence that aggrecan domains contract in the presence of a high concentration of dextran (Harper and Preston, 1987).

The formation of aggregates caused by the specific binding of many aggrecans to each hyaluronan chain (Hardingham and Muir, 1972; Hardingham, 1981) resulted in a large reduction in the lateral diffusion coefficient (Fig. 5), which is compatible with previous physical assessments of this aggregation process (Reihanion et al., 1979). The MALLS data suggest that aggregates contain ~30 monomers. Therefore, given a monomer D_o of 4.25×10^{-8} cm^2 s^{-1}, Eq. 4 predicts a D_o of 1.4×10^{-8} cm^2 s^{-1} for aggregates conforming to a spherical nonfree draining model, which is 10 times higher than would be calculated by summation for a free draining aggregate. The measured D_o (6.6×10^{-9} cm^2 s^{-1}) is intermediate between these two values and suggests a partial free draining structure, which is compatible with a noncompact, partially extended aggregate structure based on a central HA core filament. Interestingly, results suggest that for aggregates the onset of domain overlap interactions occurs between 1.5 and 2.0 mg/ml, as with the monomer (Fig. 6), although models predict that aggregate overlap occurs at 0.6 mg/ml (Phillips and Jansons, 1990). It was also notable that *B*, calculated from the exponential fit, is similar for aggregate (0.187) and monomer (0.180). Over the range investigated, monomer and aggregate lateral self-diffusion coefficients would therefore appear to scale identically with concentration, which is most apparent in the superimposed plots of D/D_0 (Fig. 6) for monomer and aggregate. This suggests that within the aggregate structure as concentration increases, the intermolecular interactions of monomers are similar to those of free monomers at comparable concentrations. Aggrecan domains are thus predicted to behave in a similar way as concentration increases in aggregate and monomer. The accuracy of the diffusion measurements determined by this method in concentrated polymer solutions will make it possible to fully test further models of their solution behavior.

We thank Dr. Peter Bayley (National Institute of Medical Research, Mill Hill, London) and Dr. Jim Ralphs (University of Cardiff, Cardiff, Wales) for giving advice and providing access to confocal microscopes for preliminary experiments. We also thank Dr. Peter Winlove (Imperial College, London) for helpful discussions and advice with data analysis, and Prof. Peter Garland (Institute for Cancer Research, London) for initial discussions.

We are grateful to the Wellcome Trust for support.

REFERENCES

Amu, T. C. 1982. Activation energy of diffusion for well fractionated dextrans in aqueous solutions. *Biophys. Chem.* 16:269–273.

Axelrod, D., D. E. Koppel, J. Schlessinger, E. L. Elson, and W. W. Webb. 1976. Mobility measurements by analysis of fluorescence photobleaching recovery kinetics. *Biophys. J.* 16:1055–1089.

Bayley, P. M., and B. Clough. 1995. Application of optical microscopy to cellular-dynamics: studies of fluorescence photobleaching (FRAP) of erythrocyte-membrane proteins using the confocal microscope. *J. Trace Microprobe Tech.* 13:209–216.

Blonk, J. C. G., A. Don, H. Van Aalst, and J. J. Birmingham. 1993. Fluorescence photobleaching in the confocal scanning light microscope. *J. Microsc.* 169:363–374.

Chen, H., J. R. Swedlow, M. Grote, J. W. Sedat, and D. A. Agard. 1995. The collection, processing and display of 3-dimensional images of biological specimens. *In* Handbook of Biological Confocal Microscopy. J. B. Pawley, editor. Plenum, New York. 197–210.

CRC Press. 1968. CRC Handbook of Biochemistry, 1st Ed. CRC Press, Boca Raton, FL.

Cutts, L. S., P. A. Roberts, J. Alder, M. C. Davies, and C. D. Melia. 1995. Determination of localised diffusion coefficients in gels using confocal scanning microscopy. *J. Microsc.* 180:131–139.

de Gennes, P. G. 1974. Scaling Concepts in Polymer Physics. Cornell University Press, Ithaca, NY.

Grodzinsky, A. J. 1983. Electromechanical and physicochemical properties of connective tissue. *CRC Crit. Rev. Bioeng.* 14:133–199.

Hardingham, T. E. 1979. The role of link-protein in the structure of cartilage proteoglycan aggregates. *Biochem. J.* 177:237–247.

Hardingham, T. E. 1981. Proteoglycans: their structure, interactions and molecular organisation in cartilage. *Biochem. Soc. Trans.* 9:489–497.

Hardingham, T. E., R. J. F. Ewins, and H. Muir. 1976. Cartilage proteoglycans: structure and heterogeneity of the protein core and the effects of specific protein modifications on the binding to hyaluronate. *Biochem. J.* 157:127–143.

Hardingham, T. E., and H. Muir. 1972. The specific interaction of hyaluronic acid with cartilage proteoglycan. *Biochim. Biophys. Acta.* 279: 401–405.

Hardingham, T. E., H. Muir, M. K. Kwan, W. M. Lai, and V. C. Mow. 1987. Viscoelastic properties of proteoglycan solutions with varying proportions present as aggregates. *J. Orthop. Res.* 5:36–46.

Harper, G. S., W. D. Comper, B. N. Preston, and P. Daivies. 1985. Concentration dependence of proteoglycan diffusion. *Biopolymers.* 24: 2165–2173.

Harper, G. S., and B. N. Preston. 1987. Molecular shrinkage of proteoglycans. *J. Biol. Chem.* 262:8088–8095.

Hess, W. 1986. Self diffusion and reptation in semidilute polymer solutions. *Macromolecules.* 19:1395–1404.

Imhof, A., A. Van Blaadren, G. Maret, J. Mellema, and J. K. G. Dhont. 1994. A comparison between the long time self diffusion of and low shear viscosity of concentrated dispersions of charged colloidal silica spheres. *J. Chem. Phys.* 100:2170–2181.

Jain, R. K., R. J. Stock, S. R. Chary, and M. Rueter. 1990. Convection and diffusion measurements using fluorescence recovery after photobleaching and video image analysis: in-vitro calibration and assessment. *Microvasc. Res.* 39:77–93.

Janmey, P. A. 1993. Application of dynamic light scattering to biological systems. *In* Dynamic Light Scattering. The Method and Some Applications. W. Brown, editor. Clarendon Press, Oxford. 611–641.

Johnson, E. M., D. A. Berk, R. J. Jain, and W. M. Deen. 1995. Diffusion and partitioning of proteins in charged agarose gels. *Biophys. J.* 68: 1561–1568.

Kitchen, R. G., and R. L. Cleland. 1978. Dilute solution properties of proteoglycan fractions from bovine nasal cartilage. *Biopolymers.* 17: 759–783.

Kubitscheck, H., P. Wedekind, and R. Peters. 1994. Lateral diffusion measurements at high spatial resolution by scanning microphotolysis in a confocal microscope. *Biophys. J.* 67:946–965.

Laurent, T. C. 1995. Structure of the extracellular matrix and the biology of hyaluronan. *In* Interstitium, Connective Tissue and Lymphatics. R. K. Reed, N. G. McHale, J. L. Bert, C. P. Winlove, and G. A. Laine, editors. Portland Press, London. 1–12.

Li, X., and W. F. Reed. 1991. Polyelectrolyte properties of proteoglycan monomers. *J. Chem. Phys* 94:4658–4580.

Mow, V. C., W. Zhu, W. M. Lai, T. E. Hardingham, C. Hughes, and H. Muir. 1989. The influence of link protein stabilisation on the viscometric properties of proteoglycan aggregate solutions. *Biochim. Biophys. Acta.* 992:201–208.

Ogston, A. G., B. N. Preston, and J. D. Wells. 1973. On the transport of compact molecules through solutions of chain polymers. *Proc. R. Soc. Lond. A.* 333:297–316.

Ohno, H., J. Blackwell, A. M. Jamieson, D. A. Caprino, and A. A. Caplan. 1986. Calibration of the relative molecular mass of proteoglycan subunit by column chromatography on Sepharose CL-2B. *Biochem. J.* 235: 553–557.

Poitevin, E., and P. Wahl. 1988. Study of the translational diffusion of macromolecules in beads of gel chromatography by the FRAP method. *Biophys. Chem.* 31:247–258.

Phillies, G. D. J. 1989. The hydrodynamic scaling model for polymer self-diffusion. *J. Phys. Chem.* 93:5029–5039.

Phillips, C. G. P., and K. M. Jansons. 1990. Flow and diffusion through random suspensions of aggregated rods: applications to proteoglycan solutions. *Macromolecules.* 23:1717–1724.

Ratcliffe, A., M. Doherty, R. N. Maini, and T. E. Hardingham. 1988. Increased concentrations of proteoglycan components in the synovial fluids of patients with acute but not chronic joint disease. *Ann. Rheum. Dis.* 57:826–832.

Reed, W. F. 1996. Data evaluation for unified multidetector size-exclusion chromatography-molar-mass, viscosity and radius of gyration. *Macromol. Chem. Phys.* 197:1539–1575.

Reihanion, H., A. M. Jamieson, L. H. Tang, and L. C. Rosenberg. 1979. Hydrodynamic properties of proteoglycan subunit from bovine nasal cartilage. Self association behaviour and interaction with hyaluronate studied by laser light scattering. *Biopolymers.* 18:1727–1747.

Schmidt, M., and W. Burchard. 1981. Translational diffusion and hydrodynamic radius of unperturbed flexible chains. *Macromolecules.* 14: 210–211.

Soumpasis, D. M. 1983. Theoretical analysis of fluorescence photobleaching recovery experiments. *Biophys. J.* 41:95–97.

Winlove, C. P., and K. H. Parker 1995. The physiological functions of extracellular matrix macromolecules. *In* Interstitium, Connective Tissue and Lymphatics. R. K. Reed, N. G. McHale, J. L. Bert, C. P. Winlove and G. A. Laine, editors. Portland Press, London. 137–165.